*Polish Journal of Chemical Technology, 17, **4**, 88 — 94, 10.1515/pjct-2015-0073*

Morphology and the physical and thermal properties of thermoplastic polyurethane reinforced with thermally reduced graphene oxide

Michał Strankowski, Łukasz Piszczyk*, Paulina Kosmela, Piotr Korzeniewski

Gdansk University of Technology, Department of Polymer Technology, Chemical Faculty, Gabriela Narutowicza Str. 11/12, 80-233 Gdansk, Poland
**Corresponding author: e-mail: lukpiszc@pg.gda.pl*

In this study, thermally reduced graphene oxide (TRG)-containing polyurethane nanocomposites were obtained by the extrusion method. The content of TRG incorporated into polyurethane elastomer systems equaled 0.5, 1.0, 2.0 and 3.0 wt%. The morphology, static and dynamic mechanical properties, and thermal stability of the modified materials were investigated. The application of TRG resulted in a visible increase in material stiffness as confirmed by the measurements of complex compression modulus (E') and glass transition temperature (T_g). The T_g increased with increasing content of nanofiller in the thermoplastic system. The addition of thermally reduced graphene oxide had a slight effect on thermal stability of the obtained materials. The incorporation of 0.5, 1.0, 2.0 and 3.0 wt% of TRG into a system resulted in increased char residues compared to unmodified PU elastomer. Also, this study demonstrated that after exceeding a specific amount of TRG, the physicomechanical properties of modified materials start to deteriorate.

Keywords: nanocomposites, graphene, polyurethane, carbon nanofillers, TRG.

INTRODUCTION

At present, nanomaterials are broadly applied due to their unique structural characteristics. Scientists mainly investigate the materials with improved physicochemical properties, which are used in the fields of nanoscience and technology. Thus the discovery of graphene and the creation of graphene-based composites significantly supplements nanoscience and plays an important role in modern technology[1]. At present, most scientific studies focus on the composites of natural origin such as montmorillonite, which is a phyllosilicate, or synthetic clays[2–6]. Clay minerals are not characterized by good conductivity and thermal properties[7] thus the use of carbon-containing nanofillers, e.g. carbon black, expanded graphite and carbon nanotubes (CNTs) may enable novel applications[8–10]. CNTs are among carbon nanofillers that have the most effective conductivity[11]. However, it is not economic to use CNTs in polymeric composites due to high production costs[12]. Graphene is another carbon nanofiller. Graphene, a single atomic layer of sp2 hybridized carbon arranged in a honeycomb structure, draws immense attention because of its thermal, mechanical and electrical properties[13]. It is considered the thinnest material in the universe, with a huge applicative potential[14, 15]. The use of graphene as a nanofiller may be advantageous in comparison to other conventional nanoparticles (Na-MMT, LDH, CNT, EG) due to its large surface area, tensile strength (TS), thermal and electrical conductivity, EMI shielding capabilities, elasticity and transparency. The level of material improvement is directly related to the degree of nanofiller dispersion in polymeric matrix[16–18]. In order to produce polymeric materials with high efficiency and good graphene dispersion in the matrix, it is necessary to use additional factors, i.e. surfactants and polyelectrolytes which improve exfoliation[19, 20]. It is common knowledge that covalent bonds between graphene and polymer improve the nanocomposite properties to a much higher degree than simple physical interactions between these two components. The modified materials display significantly improved mechanical and thermal properties[21–23], better shape-memory effect[24, 25], EMI shielding capabilities[26], and increased thermal conductivity[27]. These important characteristics of graphene sparked immense interest with regard to its possible implementation in a number of devices[28]. PU is a widely used component of, e.g. coatings, adhesives, car tires, laminates, insulating materials in refrigerators and constructions, furniture, car parts, shoe soles, sportswear, etc.[29–34]. A number of recent studies have demonstrated that the addition of a small amount of graphene to polymeric nanocomposites significantly improves their physical, chemical and electrical properties[35–40].

EXPERIMENTAL

Material

Apilon 52DE20 granulate based on TPU ester matrix with bulk density of 1.18 g/cm^3 and Shore A hardness of 77 (A.P.I. APPLICAZIONI PLASTICHE INDUSTRIALI Spa, Italy) was used to produce the investigated nanocomposites by extrusion. The nanofiller was obtained from Natural Crystalline Flake Micro 850 graphite, with 98.5 wt% of atomic carbon and 5-μm particle size (Asbury Graphite Mills, Inc., USA). The nanofiller consisted of thermally reduced graphene oxide (TRG) obtained via the two-step synthesis. The intermediate form of oxidized graphite (GrO) was produced by the Hummers method with the use of $KMnO_4$ and mixture of H_2SO_4 and H_3PO_4 acids and was later thermally reduced to TRG at 200°C[41]. The micrographs of graphene oxide and reduced graphene oxide, used to modify polyurethane elastomer, are shown in Figure 1.

Preparation of TRG/TPUR nanocomposite

Dried PU granulate and TRG were mixed according to specified proportions in order to obtain a so-called masterbatch. Five different masterbatches were prepared that differed in relation to the final content of nanofiller in a given nanocomposite. To this end, the specified

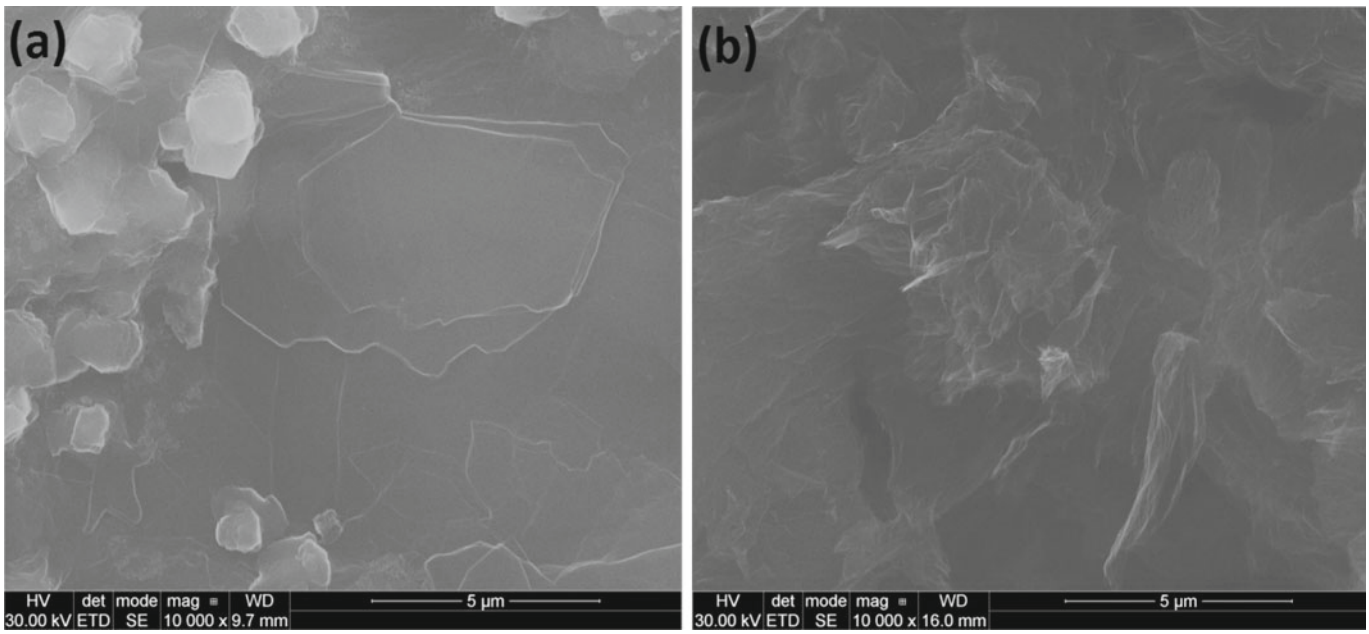

Figure 1. SEM micrographs of graphene oxide (a) and thermally reduced graphene oxide (b)

weights of granulate and TRG were mixed without any additional components (so-called dry blend) to obtain satisfactory level of homogenization. The formulations of all premixes are listed in Table 1.

Table 1. Premix formulations of TRG/TPUR nanocomposites

Premix	Weight of granulate, [g]	Weight of TRG, [g]
W_0	250.0	0
$W_{0,5}$	248.75	1.25
$W_{1.0}$	247.5	2.5
$W_{2.0}$	245.0	5.0
$W_{3.0}$	242.5	7.5

The extrusion of nanocomposites was performed by ZAMAK EHP 2×20 Sline twin screw extruder. Plastification pressure and screws rotation speed were set at 26–105 Pa and 15 rpm, respectively. The extrusion was performed at 70% of maximum load. The temperature set-points for the specific zones of electrical heater installed on the barrel are listed in Table 2.

Nanocomposite characterization

TEM analysis was performed by STEM-EDX technique, using Transmission Electron Microscope FEI Europe, Tecnai F20 X-Twin coupled with EDX Spectrometer (Samples were cut in by cryo-technique with liquid nitrogen using ultramicrotome).

The morphology of polyurethane nanocomposites was examined using a Philips-FEI XL 30 ESEM scanning electron microscope operated at 10 kV accelerating voltage.

Tensile strength tests were carried out using a Zwick/Roell Z020 universal mechanical testing machine according to PN-EN ISO 1798:2008. All series of examined materials contained five samples were cut, and the force was applied parallel to the foam rise direction. The cross head speed was set at 300 mm min^{-1} with a 5N preload.

Dynamical mechanical analysis (DMA) was performed by means of a Q800 DMA instrument (TA Instruments) at a heating rate of 4°C/min, frequency of deformation of 1 Hz and a temperature range from –80 to 120°C. The cylindrical samples were 13 mm long and 2.6 mm in diameter.

Thermogravimetric analysis (TGA) was performed on a NETZSCH TG 209 apparatus using 15-mg samples at a temperature range from 40 to 600°C and under argon atmosphere, at a heating rate of 20°C/min.

RESULTS AND DISCUSSION

The morphology of pure polyurethane and nanocomposites was examined by means of scanning electron microscopy and transmission electron microscopy. Figure 2. shows pure elastomers and nanocomposites prepared by adding 0.5, 1.0, 2.0 and 3.0 wt% of graphene. In Figure 3 the TEM micrograph of nanocomposite containing 1.0 wt% of thermally reduced graphene oxide is presented.

Figure 2. SEM images of: A – pure polyurethane elastomer (W_0), B – polyurethane elastomer containing 0.5 wt% of TRG ($W_{0.5}$), C – polyurethane elastomer filled with 1.0 wt% of TRG ($W_{1.0}$), D – polyurethane elastomer containing 2.0 wt% of TRG ($W_{2.0}$), and E – polyurethane elastomer filled with 3.0 wt% of TRG ($W_{3.0}$).

The surface morphology of fractures in the samples containing thermally reduced graphene oxide is shown in Figure 2. The neat PU showed a typical brittle fracture, and the fracture surface was smooth in this homogenous material. It is apparent from the obtained micrographs that the samples containing carbon nanofiller are characterized also by brittle fracture. At higher TRG content, nanocomposites are textured across the entire fracture surface. The roughness and much more sharp edges were seen with increasing TRG content.

Morphological TEM analysis of thermoplastic polyurethane reinforced with thermally reduced graphene oxide systems (Fig. 3) determined the nanometrical dispersion of nanoparticles in polymer matrix in samples

Table 2. Set-points of temperature zones during the extrusion

Zone number/name	Hopper	1	2	3	4	5	6	7	8	9	Connector	Extruder head
Temperature set-point ±2 [°C]	50	120	140	155	160		165				155	

MOST WIEDZY Downloaded from mostwiedzy.pl

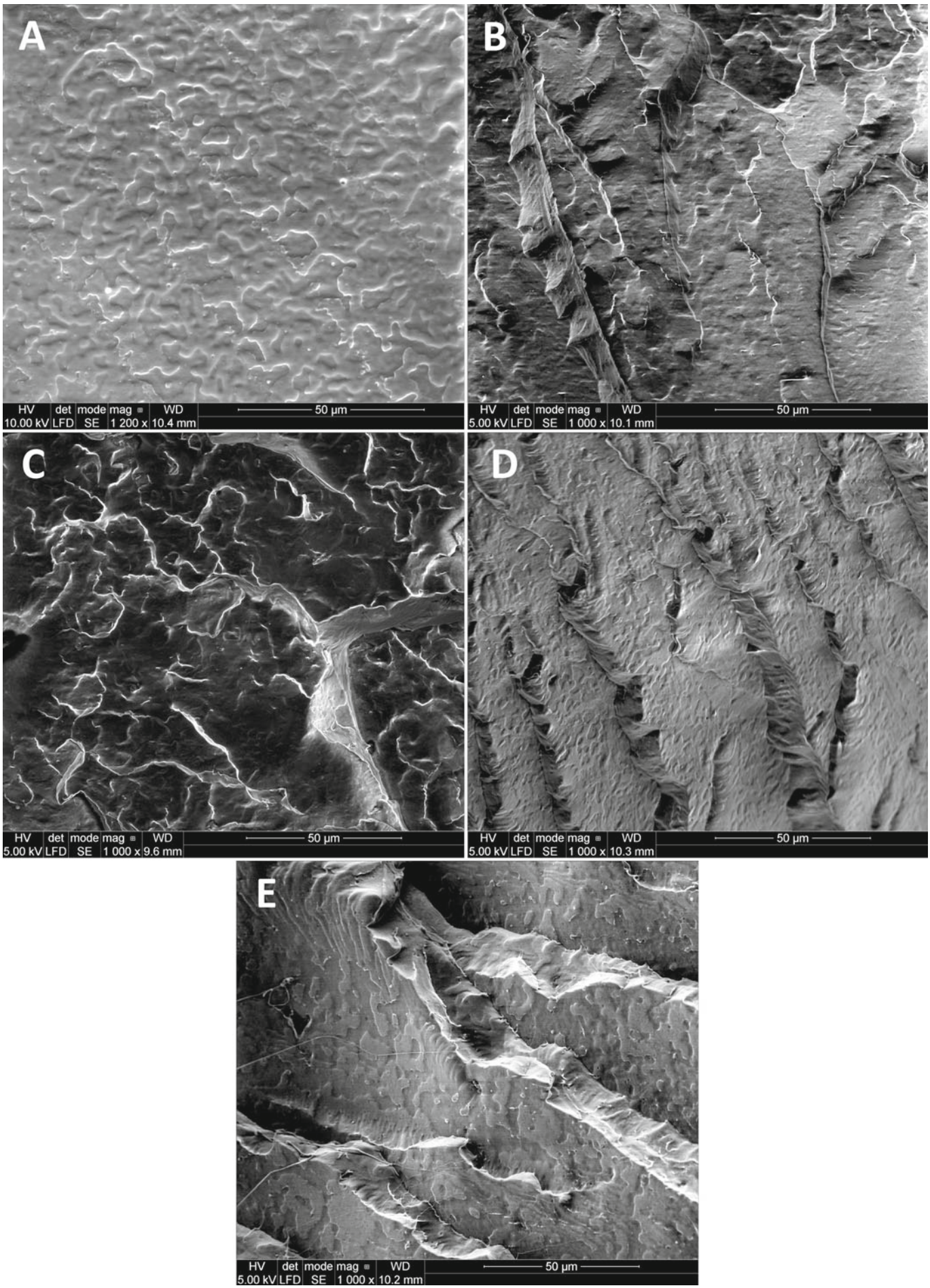

Figure 2. SEM images of: A – pure polyurethane elastomer (W_0), B – polyurethane elastomer containing 0.5 wt% of TRG ($W_{0.5}$), C – polyurethane elastomer filled with 1.0 wt% of TRG ($W_{1.0}$), D – polyurethane elastomer containing 2.0 wt% of TRG ($W_{2.0}$), and E – polyurethane elastomer filled with 3.0 wt% of TRG ($W_{3.0}$)

MOST WIEDZY Downloaded from mostwiedzy.pl

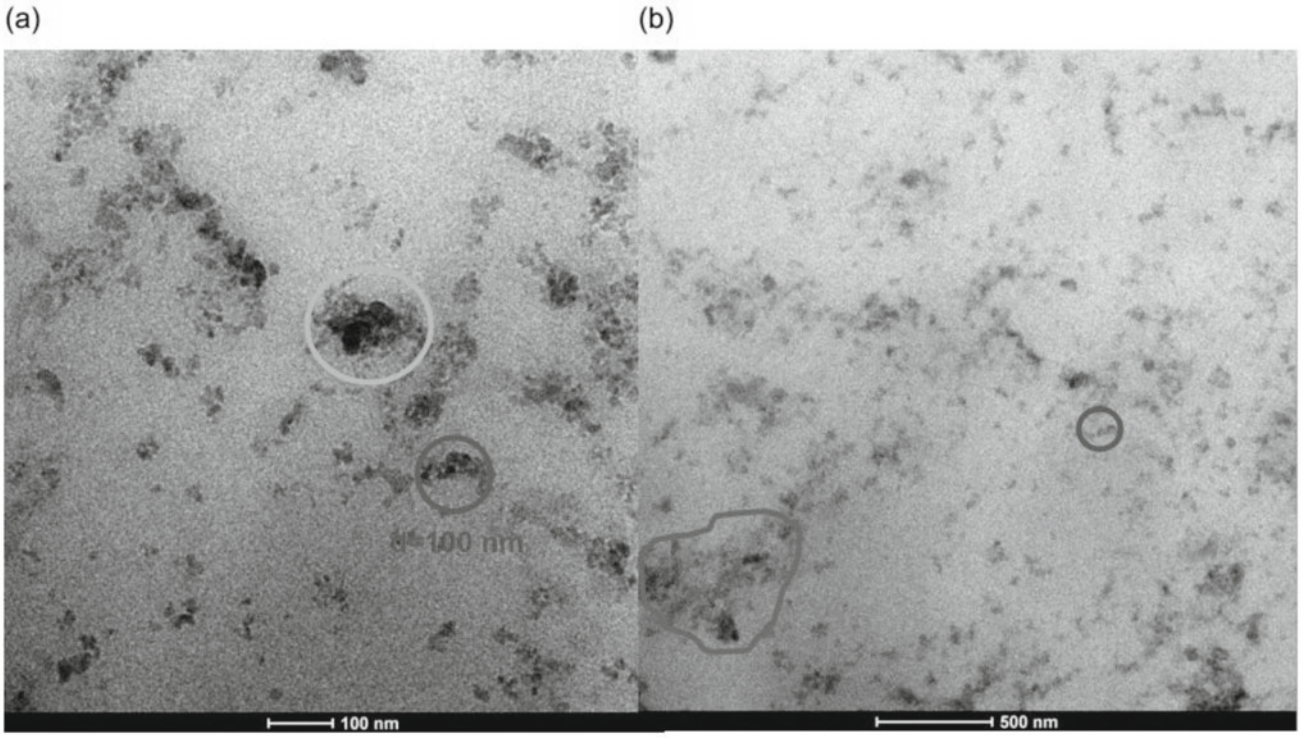

Figure 3. TEM micrographs of elastomer nanocomposite containing 1.0 wt% of thermally reduced graphene oxide at the 100 nm (A) and 500 nm scale (B)

prepared by all performed methods of nanocomponent incorporation. Nanofiller, incorporated using twin screw extruder agglomerates (in nano-scale) during synthesis processes. Filler agglomeration (10–100 nm) was also indirectly confirmed in mechanical studies analysis of nanocomposites. At higher nanofiller content, the tensile strain reduction was observed. It is important, that TEM technique gave the direct information about the morphology nanocomposite's systems. The results of the microscopic study confirmed high degree of nanofiller dispersion in polyurethane matrix.

Mechanical properties

Table 3 contains the values of tensile strength, elongation at break, glass transition temperature and elastic modulus measured at the specified temperatures. The effect of thermally reduced graphene oxide on the storage modulus (E') of PU/TRG nanocomposites in comparison to pure polyurethane is illustrated in Figure 4, while the corresponding tan δ in the function of temperature curves are presented in Figure 5.

The addition of 0.5 wt% of nanofiller resulted in a decrease in tensile strength by ca. 15% (35.5 MPa for pure PU versus 30.3 MPa for nanocomposite $W_{0.5}$) and an increase in elongation at break (867% for pure PU versus 934% for $W_{0.5}$). A similar relationship was observed in the case of nanocomposites containing 1 wt% of TRG. This phenomenon can be explained by irregular dispersion of nanofillers in polymer matrix, which might have caused the formation of carbon nanofiller aggregates that worsen mechanical properties of the final material.

The addition of nanofiller in 2 wt%, have influence in the formation of larger agglomerates in polyurethane matrix, which interact less with the polymer chains. As a result, there was a slight increase in the mechanical strength of the filled systems.

For the investigated range of temperature, all storage modulus (E') curves displayed three regions, i.e. glass transition region characterized by the reduced mobility of polymeric chains; viscoelastic region in which a significant decrease in the value of E' occurs with increasing temperature; and plastic region where the storage modulus decreases further with increasing temperature. The application of thermally reduced graphene oxide resulted in increased storage modulus in the viscoelastic region of the curve. This indicates improved stiffness of the modified material due to the presence of nanofiller in polyurethane systems, which lowers the mobility of polymeric chains.

Table 3 contains the values of storage modulus (E') at –50°C and room temperature, and the maximum temperatures of glass transition. The addition of TRG to polyurethane matrix resulted in increased storage modulus (E') compared to that of pure polyurethane. At room temperature, all TRG-modified samples were characterized by the higher values of storage modulus (E') compared to the reference sample. The observed increase in elastic modulus (Fig. 4) is in agreement with

Table 3. Static and dynamic mechanical properties of polyurethane nanocomposites

Sample	Mechanical properties				
	Tsb [MPa]	Eb [%]	T_g [°C]	$logE'_{[-50°C]}$	$logE'_{[25°C]}$
W_0	35.50 ±4,35	867 ±35	–27	1382	22
$W_{0.5}$	30.30 ±1.17	934 ±55	–18	1667	28
$W_{1.0}$	27.19 ±1.77	977 ±40	–18	2390	29
$W_{2.0}$	40.03 ±2.32	905 ±33	–18	2878	33
$W_{3.0}$	29.34 ±1.79	844 ±39	–16	3247	73

MOST WIEDZY Downloaded from mostwiedzy.pl

the known effect of carbon nanofiller on polymeric matrices[42]. The increase in the modulus of nanocomposites with the nanofiller is reasonably well understood. The reasons involve a hydrodynamic effect and adsorption of polymer chains on the filler surfaces and increase in the crosslink density by polymer/filler interaction.

Changes in the mechanical properties of polyurethane nanocomposites are strictly associated with the morphology of the materials. In the Figure 2 and Figure 3, there is shown the morphology of fracture surface and morphology of nanocomposites containing 1 wt.% of TRG. Basing on presented images, it can be seen that increasing content of nanofiller results in generation of agglomerates in polymer matrix, leading to the decrease of tensile strength. Effect of this phenomenon can be seen in the Figure 2d and 2e, where the place of brittle fracture is marked.

Glass transition temperature was determined as a maximum peak of the tanδ versus temperature curve (Fig. 5). The obtained glass transition temperatures for samples W_0, $W_{0.5}$, $W_{1.0}$, $W_{2.0}$, $W_{3.0}$ equaled –27, –18, –18, –18 and –16°C, respectively. The incorporation of thermally reduced graphene oxide into polyurethane matrix caused an upward shift in glass transition temperature. The observed temperature shift can be explained by the reduced chain mobility of soft segments due to good dispersion of carbon nanofiller in polyurethane matrix[43]. Incorporation of higher amount of TRG to polymer matrix decreased the mobility of polymer chains and resulted in the increase of the stiffness of composite, which have been shown in the Figure 4 and Table 3. This could be also interpreting as crosslinking effect of the nanofiller. Reduced graphene oxide has some reactive groups (hydroxyl or epoxy) on the surface and during processing, in molten state, these groups can react with the polymer and consequently increase crosslink density of the filled system. Shift of glass transition temperature towards higher values in case of samples containing 2 and 3 wt.% of nanofiller can be associated with the increase of the energy, which allows the material to change from glassy state to viscoelastic state.

Thermal properties

Polyurethanes degrade following a two-step process, i.e. the first step is associated with the degradation of hard segments, which depolymerize into the main monomers, while the second step is due to the decomposition of soft segments[44]. The first degradation step occurs at a temperature range from 300 to 370°C, while the second step takes place between 380 and 480°C.

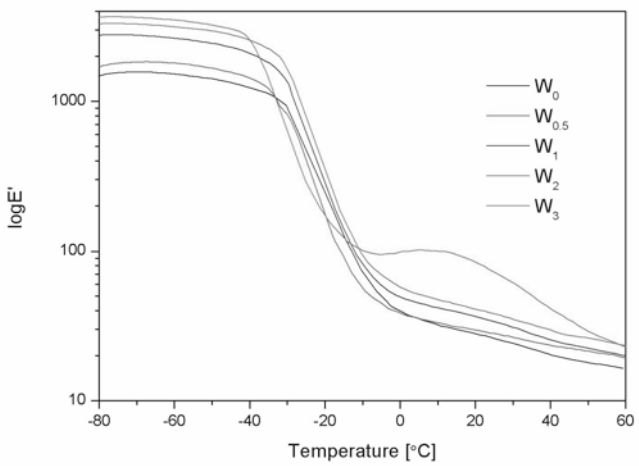

Figure 4. Storage modulus of flexible PU nanocomposite foams as a function of temperature

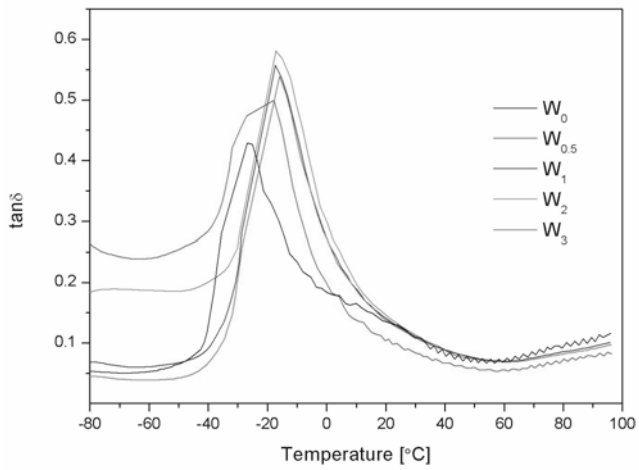

Figure 5. Damping factor (tan δ) of flexible PU nanocomposite foams as a function of temperature

The effects of TRG on thermal stability of the resulting foams were assessed by TG and derivative thermogravimetric analysis. The obtained results for the flexible polyurethane nanocomposite foams, investigated under nitrogen atmosphere, are presented in Figure 6 and 7. The temperatures at which 2, 5, 10 and 50% mass loss occurred (T_2, T_5, T_{10} and T_{50}, respectively), and the temperatures corresponding to the maximum decomposition rate (T_{max}) for the analyzed nanocomposite are listed in Table 4.

The incorporation of thermally reduced graphene oxide did not cause a large change in the temperature at which the nanocomposite decomposition starts. Moreover, with progressing decomposition at elevated temperatures, the obtained curves overlap for the entire temperature range (Fig. 6). The noticeable changes were found in the case of DTG curve where the effect of TRG addition on the decomposition rate of the obtained nanocomposites was apparent in comparison to non-modified matrix. The effect occurred at temperatures characteristic for the rigid segment decomposition (360–380°C) as well as for the degradation of residues in the second stage

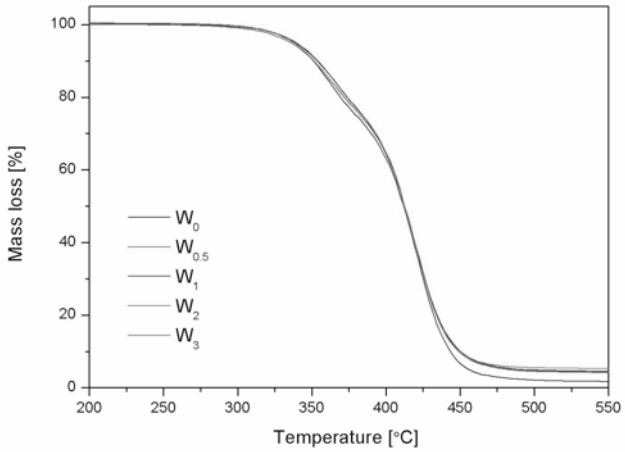

Figure 6. Mass loss versus temperature curve for polyurethane elastomers and polyurethane elastomer nanocomposites

MOST WIEDZY Downloaded from mostwiedzy.pl

Table 4. Temperatures at which 2, 5, 10 and 50% mass loss occurred and the temperature corresponding to the maximum decomposition rate (T_{max}) for different nanocomposite samples

Sample	Degradation temperature						Char residue, [%]
	T_2,[°C]	T_5,[°C]	T_{10},[°C]	T_{50},[°C]	T_{max1},[°C]	T_{max2},[°C]	
W_0	336	337	351	411	364	421	1.64
$W_{0.5}$	337	339	353	412	369	419	4.04
$W_{1.0}$	335	339	353	412	368	420	4.26
$W_{2.0}$	331	335	351	412	366	422	3.86
$W_{3.0}$	331	337	351	412	359	420	4.63

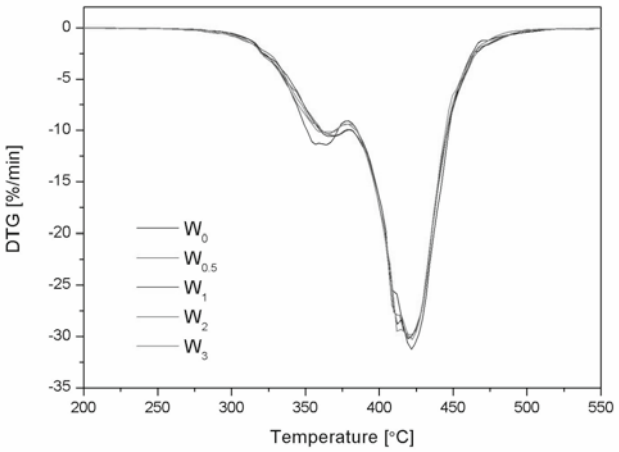

Figure 7. Differential thermogravimetric curve for pure polyurethane elastomers and polyurethane elastomer nanocomposites

(410–430°C). The incorporation of 0.5 wt% of TRG resulted in the upward shift of T_{max1} by 5°C compared to the reference sample. It was also noticed that the amount of ash increased, which may indicate that only matrix had decomposed. The amount of residue, which increases with increasing content of nanofiller, to a large extent consisted of the nanofiller that had not undergone decomposition at the highest temperature applied.

CONCLUSIONS

The presented results demonstrate that the incorporation of thermally reduced graphene oxide into the polyurethane structure by the extrusion method results in a change in mechanical properties of the obtained systems. The conducted dynamical analysis allows us to conclude that after exceeding a certain minimum amount of nanofiller the changes in the material's elastic properties occur in both glass transition and rubber elasticity regions. This is due to the high activity of nanofiller surface, correlated to the large surface area of nanofiller relative to its mass, which allows for the occurrence of additional interactions between nanofiller and matrix.

Based on static analysis of stretched nanocomposites, it can be concluded that there is a certain level of filling for which the PU/TRG nanocomposite weakens, and thus a lower stretching force is required to break it. This effect is related to increased number of nanofiller agglomerates due to increasing degree of matrix filling, as confirmed by TEM analysis.

Considering thermal stability, the application of nanofiller only enabled a decrease in the mass loss rate at both decomposition steps of hard segments and the remaining residues. However, the added nanofiller did not raise the temperature at which degradation starts, which is a key parameter used to define flammability of a given material.

ACKNOWLEDGMENT

This work was supported by the National Research and Development Centre, Poland. Project No GRAF-TECH/NCBR/11/08/2013, „Polyurethane nanocomposites containing reduced graphene oxide" implemented under the acronym „PUR-GRAF.

LITERATURE CITED

1. Stankovich, S., Dikin, D.A., Dommett G.H.B., Kohlhaas K.M., Zimney E.J. & Stach E.A., et al. (2006). Graphene-based composite materials. *Nature* 442, 282–286. DOI: 10.1038/nature04969.
2. Ray, S.S. & Okamoto, M. (2003). Polymer/layered silicate nanocomposites: a review from preparation to processing. *Prog. Polym. Sci.* 28, 1539–1641. DOI: 10.1016/j.progpolymsci.2003.08.002.
3. Leroux, F. & Besse, J.P. (2001). Polymer intercalated layered double hydroxide: a new emerging class of nanocomposites. *Chem. Mater.* 13, 3507–3515. DOI: 10.1021/cm0110268.
4. Peng, L., Kim, N.H., Bhadra, S. & Lee, J.H. (2009). Electroresponsive property of novel poly(acrylate-acryloyloxyethyl trimethyl ammoniumchloride)/clay nanocomposite hydrogels. *Adv. Mater. Res.* 79, 2263–2266. DOI: 10.4028/www.scientific.net/AMR.79-82.2263.
5. Giannelis, E.P., Krishnamoorti, R. & Manias, E. (1999). Polymer-silicate nanocomposites: model systems for confined polymers and polymer brushes. *Adv. Polym. Sci.* 138, 107–147. DOI: 10.1007/3-540-69711-X_3.
6. Uddin, F. (2008). Clays, nanoclays, and montmorillonite minerals. *Metall. Mater. Trans. A* 39, 2805–2814. DOI: 10.1007/s11661-008-9603-5.
7. Zhang, W., Blackburn, R.S. & Dehghani-Sanij, A. (2007). Electrical conductivity of epoxy resin-carbon black-silica nanocomposites: effect of silica concentration and analysis of polymer curing reaction by FTIR. *Scripta. Mater.* 57, 949–952. DOI: 10.1016/j.scriptamat.2007.07.030.
8. Li, Q., Siddaramaiah, Kim, N.H., Yoo, G.H. & Lee, J.H. (2009). Positive temperature coefficient characteristic and structure of graphite nanofibers rein- forced high-density polyethylene/carbon black nanocomposites. *Compos. Part B* 40, 218–224. DOI: 10.1016/j.compositesb.2008.11.002.
9. Chen, X., Zheng, Y.P., Kang, F. & Shen, W.C. (2006). Preparation and structure analysis of carbon/carbon composite made from phenolic resin impregnation into exfoliated graphite. *J. Phys. Chem. Solids* 67, 1141–1144. DOI: 10.1016/j.jpcs.2006.01.087.
10. Liao, S.H., Yen, C.Y., Weng, C.C., Lin, Y.F., Ma, C.C.M. &Yang, C.H., et al. (2008). Preparation and properties of carbon nanotube/polypropylene nanocomposite bipolar plates for polymer electrolyte membrane fuel cells. *J. Power. Sources.* 185, 1225–1232. DOI: 10.1016/j.jpowsour.2009.06.064.
11. Liu, N., Luo, F., Wu, H., Liu, Y., Zhang, C. & Chen, J. (2008). One step ionic-liquid-assisted electrochemical

MOST WIEDZY Downloaded from mostwiedzy.pl

synthesis of ionic-liquid-functionalized graphene sheets directly from graphene. *Adv. Funct. Mater.* 18, 1518–1525. DOI: 10.1002/adfm.200700797.
12. Zhu, Y., Murali, S., Cai, W., Li, X., Suk, J.W. & Potts, J.R., et al. (2010). Graphene and graphene oxide: Synthesis, properties, and applications. *Adv. Mater.* 22, 3906–3924. DOI: 10.1002/adma.201001068.
13. Si, Y. & Samulski, T. (2008). Synthesis of water soluble graphene. *Nano. Lett.* 8, 1679–1682. DOI: 10.1021/nl080604h.
14. Geim, A.K. & MacDonald, A.H. (2007). Graphene: exploring carbon flatland. *Phys. Today* 60(8), 35–34. DOI: 10.1063/1.2774096.
15. Wang, G., Shen, X., Wang, B., Yao, J. & Park, J. (2009) Synthesis and characterization of hydrophilic and organophilic graphene nanosheets. *Carbon* 47, 1359–1364. DOI: 10.1016/j.carbon.2009.01.027.
16. Wang, G., Yang, J., Park, J., Gou, X., Wang, B. & Liu, H., et al. (2008). Facile synthesis and characterization of graphene nanosheets. *J. Phys. Chem. C* 112, 8192–8195. DOI: 10.1021/jp710931h.
17. Dreyer, R.D., Park, S., Bielawski, C.W. & Ruoff, R.S. (2010). The chemistry of graphene oxide. *Chem. Soc. Rev.* 39, 228–240. DOI: 10.1039/b917103g.
18. Wang, X., Yang, H., Song, L., Hu, Y., Xing, W. & Lu, H. (2011). Morphology, mechanical and thermal properties ofgraphene-reinforced poly(butylene succinate) nanocomposites. *Compos. Sci. Technol*. 72, 1–6. DOI: 10.1016/j.compscitech.2011.05.007.
19. Kim, H., Abdala, A.A. & Macosko, C.W. (2010). Graphene/polymer nanocomposites. *Macromolecules* 43, 6515–6530. DOI: 10.1021/ma100572e.
20. Mya, K.Y., Gose, H.B., Pretsch, T., Bothe, M. & He, C. (2011). Star-shaped POSS-polycaprolactone polyurethanes and their shape memory performance. *J. Mater. Chem.* 21, 4827–4836. DOI: 10.1039/C0JM04459H.
21. Ma, W.S., Wu, L., Yang, F. & Wang, S.F. (2014). Non-covalently modified reduced graphene oxide/polyurethane nanocomposites with good mechanical and thermal properties. *J. Mater. Sci.* 49, 562–571. DOI: 10.1007/s10853-013-7736-4.
22. Jung, Y.C., Sahoo, N.G. & Cho, J.W. (2006). Polymeric nanocomposites of polyurethane block copolymers and functionalized multi-walled carbon nanotubes as crosslinkers. *Macromol Rapid Commun.* 27, 126–131. DOI: 10.1002/marc.200500658.
23. Kim, J.T., Kim, B.K., Kim, E.Y., Park, H.C. & Jeong, H.M. (2014). Synthesis and shape memory performance of polyurethane/graphene nanocomposites. *Reac. Func. Polym.* 74, 16–21. DOI: 10.1016/j.reactfunctpolym.2013.10.004.
24. Park, J.H. & Kim, B.K. (2014). Infrared light actuated shape memory effects in crystalline polyurethane/graphene chemical hybrids. *Smart Mater. Struct.* 23, from http://iopscience.iop.org/0964-1726/23/2/025038, DOI: 10.1088/0964-1726/23/2/025038.
25. Bernal, M.M., Martin-Gallego, M., Molenberg, I., Huynen, I., L´opez, M.A. & Verdejo, M.R. (2014). Influence of carbon nanoparticles on the polymerization and EMI shielding properties of PU nanocomposite foams. *RSC Adv.* 4, 7911–7918. DOI: 10.1039/C3RA45607B.
26. Hodlur, R.M. & Rabinal, M.K. (2014). Self assembled graphene layers on polyurethane foam as a highly pressure sensitive conducting composite. *Compos. Sci. Technol.* 90, 160–165. DOI: 10.1016/j.compscitech.2013.11.005.
27. Allen, M.J., Tung, V.C. & Kaner, R.B. (2010). Honeycomb carbon: a review of grapheme. *Chem. Rev.* 110, 132–145. DOI: 10.1021/cr900070d.
28. Delebecq, E., Pascault, J.P., Boutevin, B. & Ganachaud, F. (2013). On the versatility of urethane/urea bonds: reversibility, blocked isocyanate, and non-isocyanate polyurethane. *Chem. Rev.* 113, 80–118. DOI: 10.1021/cr300195n.
29. Sadasivuni, K.K., Ponnamma, D., Thomas, S. & Grohens, Y. (2014). Evolution from graphite to graphene elastomer composites. *Prog. Polym. Sci.* 39, 749–780. DOI: 10.1016/j.progpolymsci.2013.08.003.
30. Huang, X., Qi, X., Boey, F. & Zhang, H. (2012). Graphene-based composites. *Chem. Soc. Rev.* 41, 666–686. DOI: 10.1039/C1CS15078B.
31. Jung, Y.C., Yoo, H.J., Kim, Y.A., Cho, J.W. & Endo, M. (2010). Electroactive shape memory performance of polyurethane composite having homogeneously dispersed and covalently crosslinked carbon nanotubes, *Carbon* 48, 1598–1603. DOI:10.1016/j.carbon.2009.12.058.
32. Yadav, S.K., Mahapatra, S.S. & Cho, J.W. (2012). Synthesis of mechanically robust antimicrobial nanocomposites by click coupling of hyperbranched polyurethane and carbon nanotubes, *Polymer* 53, 2023–2031. DOI: 10.1016/j.polymer.2012.03.010.
33. Deka, H., Karak, N., Kalita, R.D. & Buragohain, A.K. (2010). Biocompatible hyperbranched polyurethane/multi-walled carbon nanotube composites as shape memory materials. *Carbon* 48, 2013–2022. DOI: 10.1016/j.carbon.2010.02.009.
34. Ma, W.S., Wu, L., Yang, F. & Wang, S.F. (2014). Non-covalently modified reduced graphene oxide/polyurethane nanocomposites with good mechanical and thermal properties. *J. Mater. Sci.* 49, 562–571. DOI: 10.1007/s10853-013-7736-4.
35. Cai, D., Yusoh, K. & Song, M. (2009). The mechanical properties and morphology of a graphite oxide nanoplatelet/polyurethane composite. *Nanotechnology* 20, from http://iopscience.iop.org/0957-4484/20/8/085712. DOI: 10.1088/0957-4484/20/8/085712.
36. Bernal, M.M., Molenberg, I., Estravis, S., Rodriguez-Perez, M.A., Huynen, I., Lopez-Manchado, M.A. & Verdejo, R. (2012). Comparing the effect of carbon-based nanofillers on the physical properties of flexible polyurethane foams. *J. Mater. Sci.* 47, 5673–5679. DOI: 10.1007/s10853-012-6331-4.
37. Mya, K.Y., Gose, H.B., Pretsch, T., Bothe, M. & He, C. (2011). Star-shaped POSS-polycaprolactone polyurethanes and their shape memory performance. *J. Mater. Chem.* 21, 4827–4836. DOI: 10.1039/C0JM04459H.
38. Park, J.H. & Kim, B.K. (2014). Infrared light actuated shape memory effects in crystalline polyurethane/graphene chemical hybrids. *Smart Mater. Struct.* 23, 1–7. DOI: 10.1088/0964-1726/23/2/025038.
39. Bernal, M.M., Molenberg, I., Estravis, S., Rodriguez-Perez, M.A., Huynen, I., Lopez-Manchado, M.A. & Verdejo, R. (2012). Comparing the effect of carbon-based nanofillers on the physical properties of flexible polyurethane foams. *J. Mater. Sci.* 47, 5673–5679. DOI: 10.1007/s10853-012-6331-4.
40. Hodlur, R.M. & Rabinal, M.K. (2014). Self assembled graphene layers on polyurethane foam as a highly pressure sensitive conducting composite. *Compos. Sci. Technol.* 90, 160–165. DOI: 10.1016/j.compscitech.2013.11.005.
41. Cai, D., Yusoh, K. & Song, M. (2009). The mechanical properties and morphology of a graphite oxide nanoplatelet/polyurethane composite. Nanotechnology 20, from http://iopscience.iop.org/0957-4484/20/8/085712. DOI: 10.1088/0957-4484/20/8/085712.
42. Xia, H.S. & Song, M. (2005). Preparation and characterization of polyurethane–carbon nanotube Composites. *Soft Matter* 1(5), 386–394. DOI: 10.1039/b509038e.
43. Chattopadhyay, D.K. & Webster, D.C. (2009) . Thermal stability and flame retardancy of polyurethanes. Prog. Polym. Sci. 34(10), 1068–1133. DOI: 10.1016/j.progpolymsci.2009.06.002.
44. Thirumal, M., Khastgir, D., Nando, G.B., Naik, Y.P. & Singha, N.K. (2010). Halogen-free flame retardant PUF: effect of melamine compounds on mechanical, thermal and flame retardant properties. *Polym. Degrad. Stab.* 95(6), 1138–1145. DOI: 10.1016/j.polymdegradstab.2010.01.035.

MOST WIEDZY Downloaded from mostwiedzy.pl